JOURNAL OF VIROLOGY, Apr. 2005, p. 5017–5026 Vol. 79, No. 8
0022-538X/05/$08.00+0 doi:10.1128/JVI.79.8.5017–5026.2005

Penetration of Enveloped Double-Stranded RNA Bacteriophages ϕ13 and ϕ6 into *Pseudomonas syringae* Cells

Rimantas Daugelavičius,[1,2] Virginija Cvirkaitė,[1,2] Aušra Gaidelytė,[1,2] Elena Bakienė,[2] Rasa Gabrėnaitė-Verkhovskaya,[1]† and Dennis H. Bamford[1]*

Department of Biological and Environmental Sciences and Institute of Biotechnology, University of Helsinki, Helsinki, Finland,[1] and Department of Biochemistry and Biophysics, Vilnius University, Vilnius, Lithuania[2]

Received 20 September 2004/Accepted 22 November 2004

Bacteriophages ϕ6 and ϕ13 are related enveloped double-stranded RNA viruses that infect gram-negative *Pseudomonas syringae* cells. ϕ6 uses a pilus as a receptor, and ϕ13 attaches to the host lipopolysaccharide. We compared the entry-related events of these two viruses, including receptor binding, envelope fusion, peptidoglycan penetration, and passage through the plasma membrane. The infection-related events are dependent on the multiplicity of infection in the case of ϕ13 but not with ϕ6. A temporal increase of host outer membrane permeability to lipophilic ions was observed from 1.5 to 4 min postinfection in both virus infections. This enhanced permeability period coincided with the fast dilution of octadecyl rhodamine B-labeled virus-associated lipid molecules. This result is in agreement with membrane fusion, and the presence of temporal virus-derived membrane patches on the outer membrane. Similar to ϕ6, ϕ13 contains a thermosensitive lytic enzyme involved in peptidoglycan penetration. The phage entry also caused a limited depolarization of the plasma membrane. Inhibition of host respiration considerably decreased the efficiency of irreversible virus binding and membrane fusion. An active role of cell energy metabolism in restoring the infection-induced defects in the cell envelope was also observed.

During infection many bacteriophages deliver only their nucleic acid, leaving the virus capsid outside (for a review, see reference 42). Double-stranded RNA (dsRNA) viruses must also bring virion-associated RNA-dependent RNA polymerases into the cell, since cells do not possess enzymes that are capable of transcribing and replicating viral dsRNA templates. Accordingly, the infection mechanisms of dsRNA bacteriophages differ considerably from bacteriophages that bring only their genome into the host cytosol.

The RNA-dependent RNA polymerase of ϕ6, a dsRNA bacteriophage belonging to the *Cystoviridae* family, is a component of the viral polyhedral inner capsid (core or polymerase complex), which is surrounded by a shell of protein P8 making the nucleocapsid (NC) (10). ϕ6 has a lipid-protein envelope that surrounds the NC (28, 50). Bacteriophage ϕ6 was initially isolated by using *Pseudomonas syringae* pathovar phaseolicola (50), but it is able to infect several other *P. syringae* pathovars (14). The primary receptor of ϕ6 is a chromosomally encoded type IV pilus of *P. syringae* (2, 50). The host bacteria use these pili to adsorb to the leaf surface of the target plant (44, 45). In contrast to filamentous single-stranded DNA phages that attach to the pilus tip, many RNA phages, such as bacteriophage ϕ6, attach to the sides of the pilus. ϕ6 attaches to the pilus with its spike protein P3 (34, 44, 45).

To carry the viral polymerase complex into the host cytoplasm, ϕ6 must traverse the gram-negative cell's envelope, a multilayer barrier composed of the outer membrane (OM), the peptidoglycan layer in the periplasm, and the plasma membrane (PM). The integral phage envelope protein P6 mediates the fusion between the viral membrane and the OM. The fusion leads to the release of the phage NC into the periplasm without leakage of periplasmic markers (4). The NC-associated peptidoglycan-digesting endopeptidase P5 is required to deliver the viral core across the peptidoglycan layer (12, 35). During the final stage of entry, NC penetrates the PM to release the viral core into the host cytosol. This event is assisted by the NC surface protein P8 (2, 25, 41, 46). Based on electron microscopic data, penetration of the NC particle into the cytosol occurs via a membrane invagination and an intracellular vesicle, a process similar to endocytic entry of animal viruses (40, 48). The actual mechanisms of how the NC-containing PM vesicle is pinched off into the cytosol and how the NC is uncoated are currently not known. However, the membrane voltage ($\Delta\psi$) plays a key role in this process (41). The ϕ6 entry mechanism is unique among prokaryotes and in many aspects resembles the penetration mechanisms used by both enveloped and nonenveloped animal viruses (20, 40, 48), such as ϕ6 membrane fusion with the host OM (4), and endocytosis, as the pathway for NC penetration (41, 46).

Bacteriophage ϕ13 was isolated from the leaves of the radish plant (*Raphanus sativum*) (36). Based on cryo-electron microscopy, the ϕ13 virion is very similar to that of ϕ6 (51). The diameter of both virions is ~86 nm, and the NCs appear as ~58 nm-diameter particles. Spikes protrude from the enveloped surface of both virions. The genome organization of ϕ13 is also similar to bacteriophage ϕ6, and there are similarities in the amino acid sequences of some proteins. However, the products of genes 3, 5, 9, and 10 have no detectable similarity to the corresponding proteins in ϕ6 (43).

The preliminary morphological analysis of cells infected with

* Corresponding author. Mailing address: Viikki Biocenter, P.O. Box 56 (Viikinkaari 5) FI-00014, University of Helsinki, Helsinki, Finland. Phone: 358-9-191-59100. Fax: 358-9-191-59098. E-mail: dennis.bamford@helsinki.fi.

† Present address: Department of Applied Biology, University of Helsinki, Helsinki, Finland.

ϕ13 also indicates that it uses an entry mechanism similar to that of ϕ6. However, the Mindich laboratory (36) showed that these viruses use an lipopolysaccharide (LPS) receptor. Phage ϕ13 does not infect the normal ϕ6 host but is able to infect a strain that is resistant to ϕ6 with no type IV pilus but with a truncated O chain of LPS (36).

In addition to ϕ6-mediated envelope fusion, many gram-negative bacteria release OM vesicles packed with periplasmic components (6, 23). These vesicles are able to fuse with the OM of the target cell and introduce their content into the periplasm. In this case two LPS-covered membrane surfaces come into contact and fuse. Small unilamellar phospholipid vesicles are also able to fuse with the surface of gram-negative bacteria but only after the cells have been treated with EDTA (33). Lipid bilayer patches in the OM and bacterial OM proteins seem to be involved in this type of fusion. The enveloped dsRNA phage fusion is unique since the viral phospholipid membrane fuses with the LPS-containing bacterial OM.

A number of fluorescent probes have been used to monitor membrane fusion events in animal virus infections (7, 49). Currently, the lipophilic fluorescent dye octadecyl rhodamine B (R18), developed by Keller et al. (27), is the most popular fluorophore used. It has been shown that R18 can be incorporated into intact virions to concentrations inducing self-quenching without redistribution of the probe into the target membrane under conditions where no fusion occurs. After fusion, the virion-bound fluorophore diffuses into the cell membrane, resulting in relief of self-quenching (24, 30, 37), and an increase in fluorescence signal is subsequently observed.

We developed an R18-based fusion assay to monitor the entry of phages ϕ6 and ϕ13. In addition, membrane-associated events during the initial stages of infection were monitored by potentiometric studies of lipophilic ion distribution to gain information on the changes in *P. syringae* envelope characteristics during ϕ6 and ϕ13 entry.

MATERIALS AND METHODS

Phage, bacterial strains, and cultivation. *P. syringae* pv. phaseolicola HB10Y and phage ϕ6 were obtained from Anne K. Vidaver in 1974 (50) and propagated in the D. H. Bamford laboratory since then. *P. syringae* strains LM2489 and LM2509 and phage ϕ13 were obtained from L. Mindich (Public Health Research Institute, Newark, N.J.). Strain LM2489 is a derivative of LM2333 which, in turn, is a mutant of HB10Y but resistant to several DNA phages and sensitive to ϕ13 (36). LM2509 is a derivative of LM2489 that is resistant to ϕ6, due to loss of the receptor (type IV pilus), but sensitive to ϕ13.

All strains were grown in Luria-Bertani (LB) medium (47) with decreased NaCl content (5 g/liter) at 28°C. Soft agar contained 7 g of agar per liter of LB medium, whereas nutrient agar contained 15 g of agar.

To obtain phage agar stocks, soft agar from semiconfluent plates was removed to a flask, and 3 ml of LB medium was added per plate. The culture was incubated for 4 h at 28°C with aeration. The debris was removed by low-speed centrifugation (Sorvall GSA rotor, 20 min at 4°C, 8,000 rpm). The titers of the obtained phage stocks were ca. 2×10^{11} and 5×10^{11} PFU/ml for ϕ13 and ϕ6, respectively.

For phage purification, host cells (*P. syringae* HB10Y for ϕ6 or *P. syringae* LM2509 for ϕ13) were grown in LB medium at 28°C with aeration to a density of $\sim 2 \times 10^8$ CFU/ml. Phage was added to obtain a multiplicity of infection (MOI) of 10. After lysis, phage particles were collected, concentrated, and purified to get a 1× purified virus preparation as previously described (5, 51). Phage titers and specific infectivities were determined after every step during virus purification. Virus suspensions were used fresh or stored at −80°C.

Phage labeling with R18. For the phage labeling with R18, the host cells were grown and infected as described above. After lysis, cell debris was removed by centrifugation (Sorvall GSA rotor, 20 min, 4°C, 8,000 rpm), and the fluorescent probe R18, dissolved in ethanol, was added to the supernatant to obtain the final probe and ethanol concentrations of 5 μM and 0.5% (vol/vol), respectively. The mixture was stirred at 4°C overnight. The phage suspension was further clarified (Sorvall GSA rotor, 15 min, 4°C, 6,000 rpm), and the purification was performed as indicated for unlabeled virus (see above). R18-labeled phage was used fresh or stored at −80°C. R18 chloride was obtained from Molecular Probes.

One-step growth experiment. The bacteria were grown in LB broth at 28°C with aeration to $\sim 1.4 \times 10^8$ CFU/ml, transferred to 24°C, grown to a density of $\sim 2 \times 10^8$ CFU/ml, and infected by using different MOIs. The turbidity of infected cultures was monitored (with or without aeration) at 24°C until lysis occurred. The cell debris was removed by low-speed centrifugation (Sorvall GSA rotor, 20 min, 5°C, 8,000 rpm), and the titer of the supernatant was determined.

ϕ13 adsorption kinetics assay. LM2489 host cells were grown to a density of $\sim 1.5 \times 10^8$ CFU/ml in LB broth at 28°C, transferred to 24°C, and grown to a density of $\sim 2 \times 10^8$ CFU/ml. Cells were then infected by adding the purified virus suspension to obtain MOIs of $\sim 10^{-5}$. An assay of unadsorbed phage particles over time was performed as described by Adams (1).

Receptor saturation assay. For the receptor saturation assay, the cells were grown to a density of $\sim 2 \times 10^8$ CFU/ml as described above and infected with MOI values between 0.1 and 1,000 in equal volumes by using a fresh purified virus preparation. After 10 min of incubation at 24°C (with aeration), the cells were collected by centrifugation (Biofuge, 13,000 rpm, 2 min) and washed once with LB medium. The number of PFU in the supernatant fractions was determined.

Assay of lytic activity. The virion-associated lytic activity was assayed on agar plates as previously described (12) with the following modifications. *P. syringae* lawns were grown overnight in 0.6% agar overlay on LB plates at 28°C. After exposure of the lawn to chloroform vapor for 30 min, several dilutions of 1× purified Triton X-100-treated phages were spotted on the lawn. After incubation of the plates at 28°C for 3 h, the lytic activity was evaluated on the basis of the formation of clear zones caused by bacterial lysis. Triton X-100-treated phages that were incubated at 43°C for 20 min to inactivate the lytic enzymes were used as negative controls.

Transmission electron microscopy. LM2509 cells were infected with ϕ13 using MOIs of 6, 15, and 30 with samples taken 7.5, 15, 30, 60, and 90 min postinfection (p.i.). The infection mixtures (3 ml) were fixed with 3% glutaraldehyde (20 min, 24°C), collected by centrifugation (Sorvall SS34 rotor, 6,000 rpm, 15 min, 4°C), washed with 1 ml of 20 mM potassium phosphate buffer (pH 7.0), and pelleted in a microcentrifuge (13,000 rpm, 1 min at 24°C). The samples for transmission electron microscopy were prepared as described by Bamford and Mindich (3). The micrographs were taken with a JEOL 1200EX II electron microscope operating at 60 kV.

Fluorescence measurements. For fluorescence measurements, bacteria were grown in LB medium at 28°C with aeration to a density of $\sim 2 \times 10^8$ CFU/ml, collected by low-speed centrifugation (Sorvall GSA rotor, 6,500 rpm 12 min at 4°C), and resuspended in 100 mM sodium phosphate buffer (pH 7.0) to obtain 2×10^{11} cells/ml. The concentrated cells were kept on ice until used (maximally 4 h). The fluorescence (the $\lambda_{emission}$ is 580 nm when the $\lambda_{excitation}$ is 550 nm) was measured by a MOS-5 spectrofluorimeter connected to a computer. Cells were added to the medium, preincubated for 5 min, before the addition of R18-labeled phage and/or other supplements. A stable fluorescence level was obtained 10 to 15 s after the addition of the R18-labeled phage. The absence of considerable amounts of soluble R18 in the medium was confirmed in experiments with the resistant cells (HB10Y for ϕ13 and LM2509 for ϕ6) in the presence of 0.5 mM EDTA.

Electrochemical measurements. The concentrations of tetraphenylphosphonium (TPP^+), phenyldicarbaundecaborane (PCB^-), and K^+ ions in the medium were monitored by selective electrodes as described previously (15–18). The measurements of ion fluxes were performed simultaneously in four reaction vessels. A typical registration course of ion movements is presented in the figures. The internal TPP^+ and K^+ concentrations were calculated from the external ones, assuming that the dimensions of *P. syringae* cells are equal to those of *Escherichia coli* cells, 120 Klett units (A_{540}) correspond to 2×10^8 cells/ml, 1.25×10^9 cells correspond to 1 mg of dry mass, and the intracellular water volume of *P. syringae* is 1.1 μl/mg of dry mass (8). The membrane voltage ($\Delta\psi$) values were calculated by using a modified Nernst equation as described previously (16, 26). Tetraphenylphosphonium chloride, polymyxin B sulfate (PMB), 7730 U of PMB base/mg), and gramicidin D (GD) were purchased from Sigma, EDTA disodium salt from Serva, potassium salt of phenyldicarbaundecaborane was synthesized and purified by A. Beganskienė (Vilnius University).

Determination of ATP content. The ATP content of the cells was determined by the luciferin-luciferase method as described previously (16). The cell suspension (50 μl) was withdrawn and mixed with 750 μl of 100 mM Tris-acetate, 2 mM

EDTA buffer (pH 7.75), and 200 μl of ATP-monitoring reagent (BioOrbit, Turku, Finland). The total ATP content of the cells was measured by adding 200 μl of ATP-releasing reagent to the bacterial suspension. Intracellular ATP concentration of the cells was calculated from the external one as described in the discussion of electrochemical measurements above.

Analytical methods. Protein concentrations were measured by using the Coomassie blue method with bovine serum albumin as the standard (9). The proteins in the phage preparations were analyzed by sodium dodecyl sulfate-polyacrylamide electrophoresis as described by Olkkonen and Bamford (39).

RESULTS

Characteristics of the ϕ13 infection cycle. The highest phage titer in a one-step growth experiment was obtained by using a cell density of 2×10^8 CFU/ml (120 Klett units) and an MOI of 10. Cell lysis started 70 min p.i. and continued for 40 to 50 min (Fig. 1A). The obtained titer of the lysate was ca. 3 to 4×10^{10} PFU/ml. On average 150 to 200 infective progeny phage particles were released per cell. Starting 35 to 40 min p.i., it was possible to induce a premature lysis of infected cells by adding EDTA (0.5 mM final concentration) and diluting the infection mixture 1:10 with distilled water. However, the first PFU in the lysate appeared almost at the same time as with normal cell lysis, as also observed with ϕ6 (50). If the infected cultures were not aerated, the cell turbidity decreased in an MOI-dependent manner (Fig. 1A). In the case of uninfected cells, lack of aeration did not induce lysis but there was only a slight increase in the turbidity.

Kinetics of the phage adsorption was determined by using very low MOIs ($\sim 10^{-5}$). We studied HB10Y cells, which are sensitive to only ϕ6 (pili and long LPS O chains); LM2489, which are sensitive to ϕ6 and ϕ13 (pili and truncated LPS); and LM2509 cells, which are sensitive to only ϕ13 (no pili and truncated LPS). LM2489 and LM2509 cells adsorbed ϕ13 particles at a similar rate (shown for LM2489 in Fig. 1B). During the first 10 min of the infection, LM2489 cells adsorbed ca. 85% of the added ϕ13 but only 40% of the ϕ6 particles (Fig. 1B). The rate of ϕ6 adsorption was the same for HB10Y and LM2489 cells. About 45% of adsorbed phage ϕ6 particles but only 3% of infective ϕ13 particles were released when infected LM2489 cells were pelleted, resuspended, and pelleted again at 10 min p.i. The adsorption rate constants (1) for ϕ6 and ϕ13 at 3 min p.i. were ca. 5×10^{-9} and 1×10^{-8}, respectively (Fig. 1B).

The maximal number of infective ϕ13 particles irreversibly bound per one LM2489 cell was around 60 and was achieved at MOI ~100 (Fig. 1C). Taking into account that the specific infectivity of 1× purified ϕ6 is as close to maximal as possible ($\sim 9 \times 10^{10}$ PFU/μg of protein; calculations were based on data from Day and Mindich [19]) and that the protein content of ϕ13 virions is the same as in ϕ6 but the specific infectivity is ~10 times lower (results not shown), we found that only about 1 of 10 of the ϕ13 particles are infectious. Noninfectious particles or some fraction of them might irreversibly bind to the cell surface and, consequently, there may be more than 60 particles bound to each cell.

ϕ13 envelope fusion and labeling of the virus. Thin sections of infected LM2489 cells showed virus particles associated with the cell surface at 7.5 min p.i. (Fig. 2A). The phage envelope fusion with the host OM can be clearly seen, and intracellular enveloped NC particles can be readily distinguished, as in the case of phage ϕ6 infection (2, 4, 41, 46). The first progeny enveloped virus particles appeared ~45 min p.i., similarly to ϕ6 (not shown).

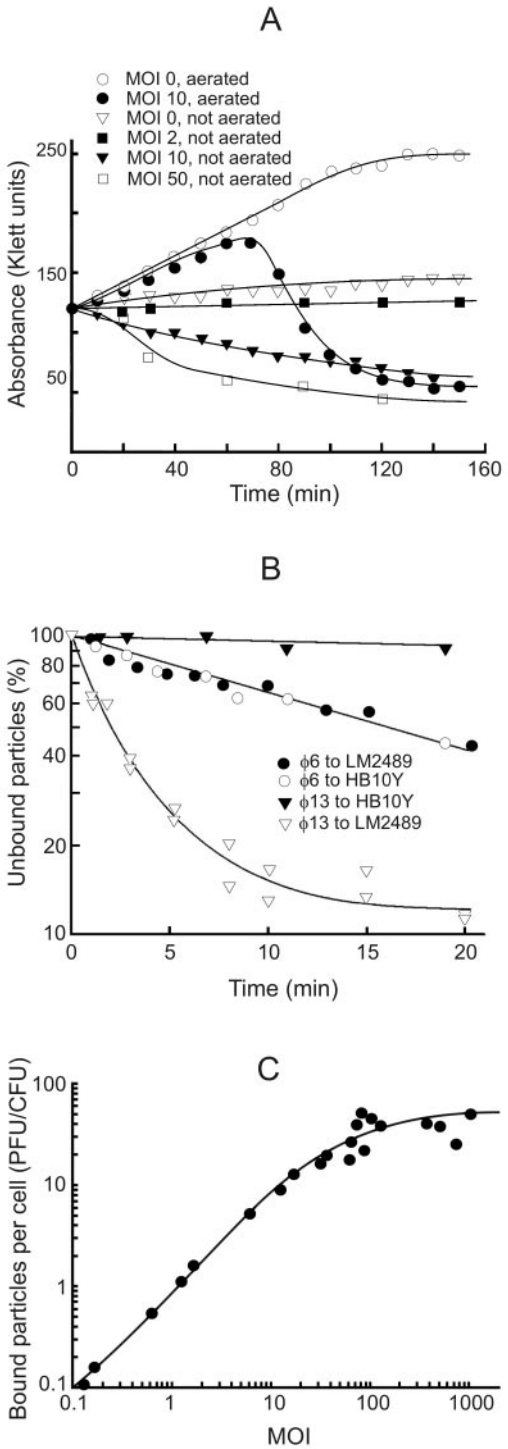

FIG. 1. Interaction of phage ϕ13 with *P. syringae* cells. Phage ϕ13 one-step growth experiments (A), phage ϕ6 and ϕ13 adsorption kinetics measurements (B), and LM2489 cell surface receptor saturation with phage ϕ13 (C). The experiments were performed as described in Materials and Methods.

Fluorescent lipid probe R18 was incorporated into phage envelopes to a high enough concentration to obtain significant

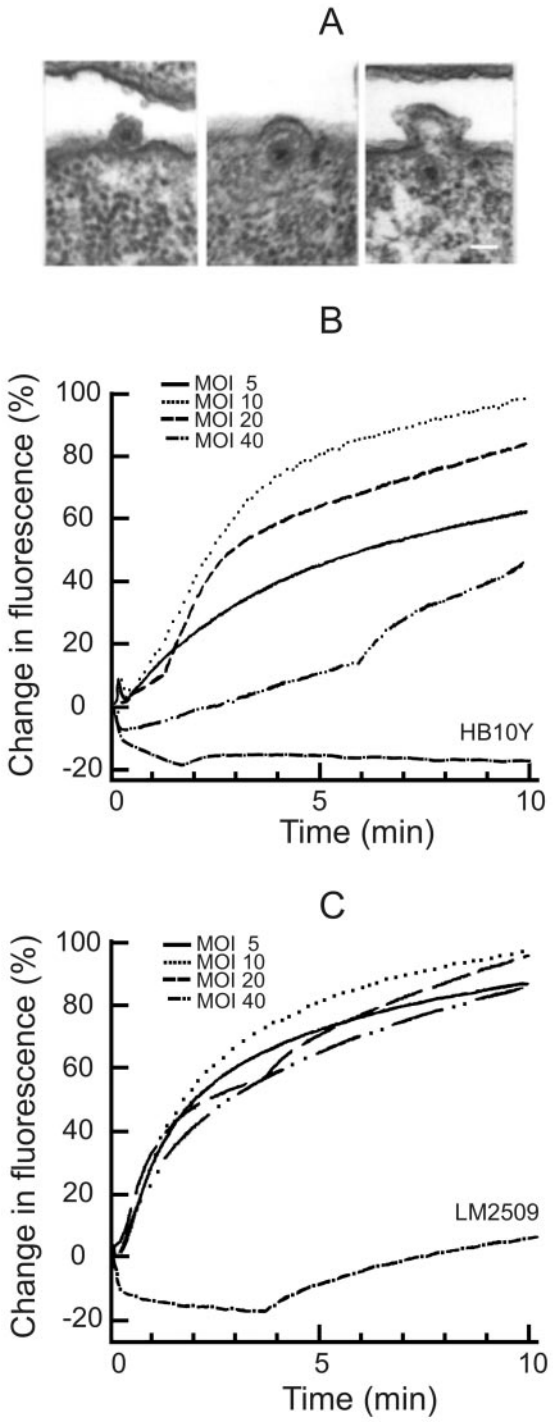

FIG. 2. Phage envelope fusion assays performed by using electron microscopy and R18 fluorescence measurements. Thin-section micrographs (A) of LM2509 cells infected with ϕ13 (MOI 15) and collected 7.5 or 15 min p.i. The scale bar represents 50 nm. (B and C) Decreased self-quenching of R18-labeled phage ϕ13 (B) and ϕ6 (C) at different MOIs. The fluorescence experiments were performed in 50 mM sodium phosphate buffer (pH 7.0), at room temperature. The MOI was changed by adding different amounts of cells (LM2509 [B]; HB10Y [C]) while using the same amount of phage particles. 100% corresponds to the fluorescence level at MOI 10 at 12 min p.i.

self-quenching. The infectivity of R18-labeled phage particles was almost equal to unlabeled ones before the purification. Although the specific infectivity of 1× purified R18-labeled ϕ6 particles was about half of the unlabeled ones, there was practically no effect of labeling in the case of ϕ13. The addition of detergent (Triton X-100) to the labeled particles caused an immediate increase in fluorescence, and approximately one-tenth of ϕ6 particles gave the same amplitude of Triton X-100-induced increase of fluorescence compared to ϕ13 (results not shown). The high accumulation of R18 into ϕ6 envelopes might explain a higher sensitivity of labeled ϕ6 particles to purification.

When labeled ϕ13 or ϕ6 particles were added to the suspension of sensitive cells, the fluorescence increase started at 10 to 15 s and leveled at 3.5 to 6 min p.i. Resistant HB10Y cells did not induce any fluorescence increase in the case of phage ϕ13. However, there was a weak late (starting ~3.5 min p.i.) increase in fluorescence after phage ϕ6 addition to LM2509 cells (Fig. 2C), although ϕ6 did not form any plaques when titers were determined on the lawn of these cells (results not shown).

Phage ϕ13 infection-induced increase of fluorescence was MOI dependent (Fig. 2B), whereas that induced by phage ϕ6 was MOI independent (Fig. 2C). The infection-induced increase of fluorescence was biphasic. An initial fast increase (~3.5 min) was followed by a slow increase (Fig. 2B and C) with similar fluorescence kinetics for both viruses.

Energy-depleting agents block ϕ6 and ϕ13 adsorption. We observed that the metabolic state of the cells affected ϕ13 adsorption. The phage bound better to fresh cells versus cells kept on ice for several hours, and the final level of fluorescence was higher when labeled phage was added to the suspension of preincubated cells compared to the situation when cells were added to the phage-containing medium. Therefore, effects of energy-depleting agents on viral adsorption and phage envelope fusion were studied. The relief of self-quenching was considerably lower when NaN_3 (blocking respiration and ATP hydrolysis by membrane H^+-ATPase) treated cells were infected with ϕ6 (Fig. 3B). However, the ϕ6 infection-induced increase in fluorescence was only slightly lower when arsenate (reducing intracellular ATP concentration by arsenolyzation of acetyl phosphates) was present. The control experiments showed that an increase in the ionic strength of the medium (addition of NaCl to 30 mM) had no considerable effect on the infection-induced increase of the fluorescence (not shown).

NaN_3 had less of an effect on the ϕ13 infection-induced increase in the fluorescence compared to ϕ6 (Fig. 3A), and arsenate had no considerable effect on membrane fusion (not shown). However, an inhibitor of cytochrome oxidase, KCN, blocked the fluorescence increase very effectively. Adsorption studies with ϕ13 confirmed the role of energy metabolism at the initial stages of infection. KCN and NaN_3 inhibited the irreversible adsorption in a concentration-dependent manner (Fig. 3C). The effects of KCN and NaN_3 on phage ϕ13 infection were stronger when the infection was performed in LB medium compared to 50 mM sodium phosphate buffer (not shown).

OM permeability and membrane voltage changes during ϕ13 and ϕ6 infections. *P. syringae* cells accumulate low amounts of TPP^+ due to the low permeability of the OM (Fig.

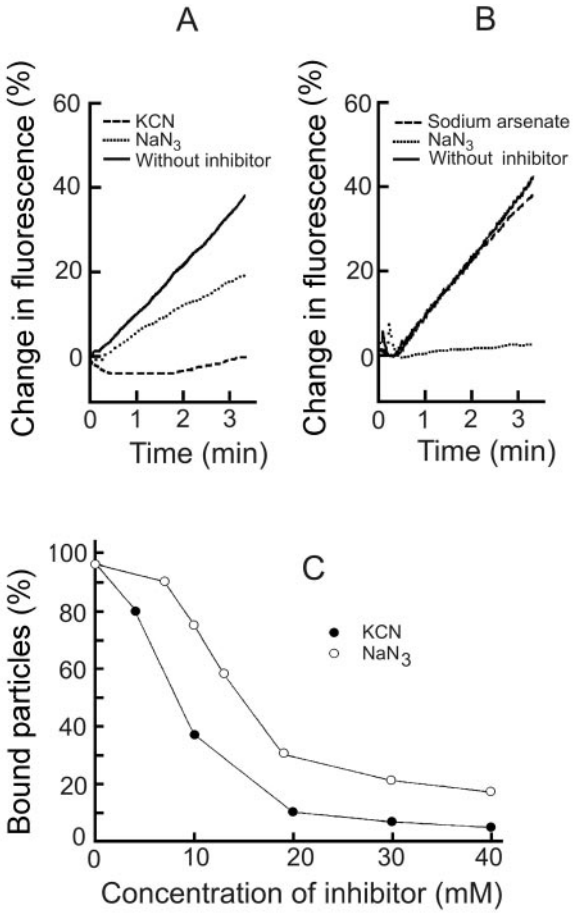

FIG. 3. Effects of energy-depleting agents on the infection-induced increase in fluorescence (A and B) and ϕ13 adsorption (C). Experiments were performed at room temperature in LB medium. LM2509 (A and C) or HB10Y (B) cells were incubated with drugs for 5 min and then infected with R18-labeled ϕ13 (A) and ϕ6 (B) or unlabeled ϕ13 (C) particles at an MOI of 10 (A and B) or 0.1 (C). (A and B) 100% indicates the level of fluorescence 12 min p.i. in the absence of drugs. The final drug concentrations were 20 mM (A and B) or as indicated (C).

4). EDTA removes divalent cations from the LPS layer, increasing the cell envelope permeability to lipophilic compounds. The treatment of *P. syringae* cells with EDTA at concentrations higher than 0.04 mM induces the uptake and distribution of TPP^+ between the cytosol and external medium according to membrane voltage ($\Delta\psi$, Fig. 4C). The maximal accumulation of TPP^+ was observed when the concentration of EDTA was >0.2 mM. *P. syringae* cells were, however, rather sensitive to this chelator. At concentrations of ≥0.7 mM, EDTA induced only a transient accumulation of TPP^+ due to a slow depolarization of the PM (not shown).

Polycationic antibiotic PMB displaces inorganic divalent cations from the outer surface of the OM. Being bulkier than cations it replaces, PMB changes the packing order of LPS and increases the permeability of the OM to a variety of molecules, including GD (17). At concentrations of >4 μg/ml PMB induced an accumulation of TPP^+ (Fig. 4D), but at 40 μg/ml and higher concentrations PMB depolarized the PM and induced a leakage of accumulated TPP^+ (results not shown).

Changing the cell/permeabilizer concentration ratio, it was possible to choose proper concentrations of EDTA or PMB to permeabilize the cells without depolarization. In the following series of experiments, we studied the fluxes of TPP^+ across the *P. syringae* envelope upon interaction with bacteriophages ϕ6 and ϕ13 (Fig. 4). The addition of phage induced a very active accumulation of TPP^+ to the phage-sensitive cells but had no effect on the resistant cells (Fig. 4A and B). This indicates that upon adsorption bacteriophages ϕ6 and ϕ13 effectively permeabilized the OM to TPP^+. The TPP^+ accumulation continued for ~3 and ~6 min with ϕ13 and ϕ6, respectively (Fig. 4A and B). If EDTA was added after the phage, it induced a leakage of accumulated TPP^+ from infected cells but caused accumulation of TPP^+ in the case of phage-resistant cells (Fig. 4A and B). The subsequent addition of the channel-forming antibiotic GD had a rather weak effect on accumulation of TPP^+ in both uninfected and infected cells. PMB addition depolarized the cells very effectively and induced a fast efflux of accumulated TPP^+. The phage-induced depolarization of the cells in the presence of EDTA was considerably stronger in the case of ϕ13 compared to ϕ6 (compare Fig. 4C and D).

Phage ϕ6 or ϕ13 and EDTA, but neither of them alone, caused leakage of TPP^+ from infected cells (Fig. 4). There are two explanations for these results. (i) Phage-induced permeabilization of the OM to TPP^+ is temporal, and TPP^+ stays locked in the cytosol of the infected cell in the absence of EDTA in spite of PM depolarization. (ii) EDTA depolarizes the PM (see above), and phages only increase the sensitivity of the cells to this compound. Experiments with low concentrations of PMB showed (Fig. 4D) that EDTA is not obligatory for the depolarizing action of phage ϕ13 but that the phage-induced increase of OM permeability to lipophilic compounds is temporal.

Physiological changes during early stages of infection. More detailed analysis of phage entry-induced changes in bacterial energetics was performed at pH 8 (Fig. 5). In spite of higher membrane voltage, ϕ13-induced accumulation of TPP^+ was less effective under these conditions (Fig. 5A). The addition of EDTA induced an additional accumulation of TPP^+ into infected cells, but leakage of accumulated TPP^+ started immediately after the second ϕ13 addition. These results indicate that a superinfection-exclusion type phenomenon is expressed only weakly during phage ϕ13 infection.

Intact *P. syringae* cells bound high amounts of PCB^-, a lipophilic anion accumulating in biological and artificial membranes (Fig. 5B). The infection-induced PCB^- binding was rather weak and proceeded simultaneously with the phage-induced permeabilization of the OM to TPP^+ (compare Fig. 5A and B). The addition of EDTA to the cell suspension caused considerably stronger binding of PCB^- than the infection (Fig. 5B, curve 2).

P. syringae cells were not able to maintain a stable concentration of intracellular K^+ in sodium phosphate buffer (Fig. 5C), and at pH 8.0 the spontaneous leakage of K^+ was stronger than at pH 7.0 (not shown). The maximal concentration of intracellular K^+ was ca. 230 mM. ϕ13 infection stimulated the K^+ leakage starting 1.5 to 2 min p.i., and the phage-stimulated leakage was observed at almost the same time period as accumulation of TPP^+ and PCB^-. The addition of EDTA very effectively depleted the intracellular K^+, and the cell depolar-

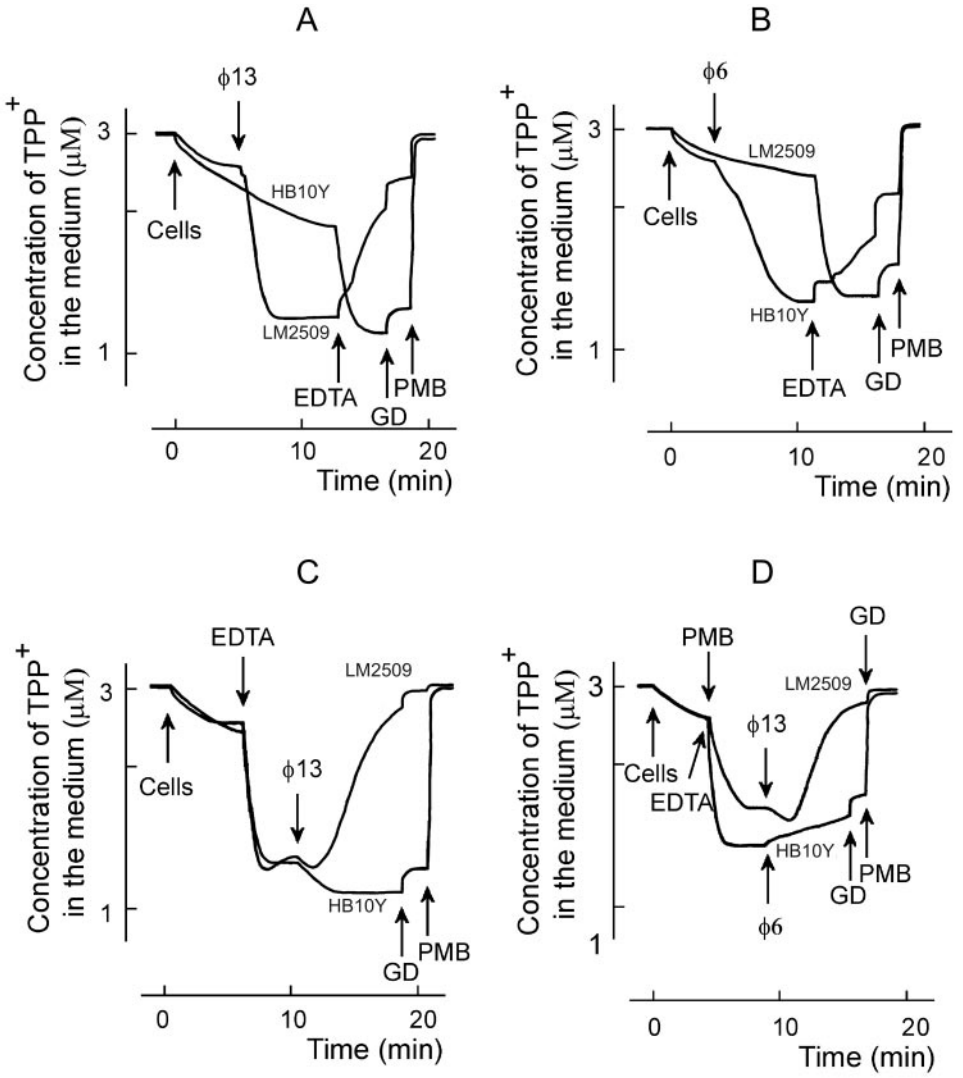

FIG. 4. Effects of phages ϕ13 (A, C, and D) or ϕ6 (B and D) on TPP^+ uptake by *P. syringae* cells. The experiments were performed at 24°C in 50 mM sodium phosphate buffer (pH 7.0) with 3×10^8 cells/ml. R18-labeled phage particles were added to obtain an MOI of 10. EDTA was used at the final concentration of 0.2 mM, and GD was used at 4 μg/ml. PMB was added to obtain the final concentration of 100 μg/ml, except for panel D, where the final PMB concentration was 5 μg/ml.

ization by GD and PMB did not have any considerable effect on K^+ equilibration between the cytosol and the medium (Fig. 5C). Phage ϕ6-induced effects on accumulation of PCB^- and K^+ were kinetically similar to those induced by ϕ13, but the amplitudes of ϕ6-induced ion fluxes were considerably weaker (results not shown).

The intracellular *P. syringae* ATP concentration was 5 to 6 mM before infection (Fig. 5D). Bacteriophages ϕ6 and ϕ13 (MOI 10) induced a small but reproducible leakage of intracellular ATP starting 1 to 1.5 min p.i. In spite of the leakage, ϕ6 infection did not considerably affect the level of ATP in the infected cells, but a decrease >50% was observed in the case of ϕ13 during the first 10 to 12 min of infection.

Prevention of virus entry by treating the virus particles at elevated temperature. In the case of ϕ6, the NC-associated lytic enzyme, digesting of a local opening in the peptidoglycan layer, is temperature sensitive (4, 12). The protein composition of ϕ13 indicates the presence of an equivalent protein (43), and we detected lytic activity associated with ϕ13 particles (not shown, but see Materials and Methods). Although only ~10% of the heat-inactivated (10 min, 30°C) phage ϕ13 particles were able to form infective centers (Fig. 6B), the fusion of viral envelope with the OM of *P. syringae* cells was not considerably affected (Fig. 6A). However, after more extensive inactivation (10 min, 35°C), ϕ13 particles were no more able to induce fluorescence increase and did not form plaques. Phage ϕ6 was less sensitive to heating, and therefore a control study was performed at temperature intervals of 23 to 50°C (Fig. 6C).

To get insights to the mechanism of heat inactivation of ϕ13 particles, the accumulation of TPP^+ by *P. syringae* during the initial stages of infection was studied (Fig. 6E). Phage ϕ13 heated 10 min at 30 or 33°C was able to induce an accumulation of TPP^+ into the host cells, indicating a normal fusion event. The final level of cell-accumulated TPP^+ in the presence of EDTA indicated that the heated phage particles did not cause a considerable PM depolarization (not shown). This

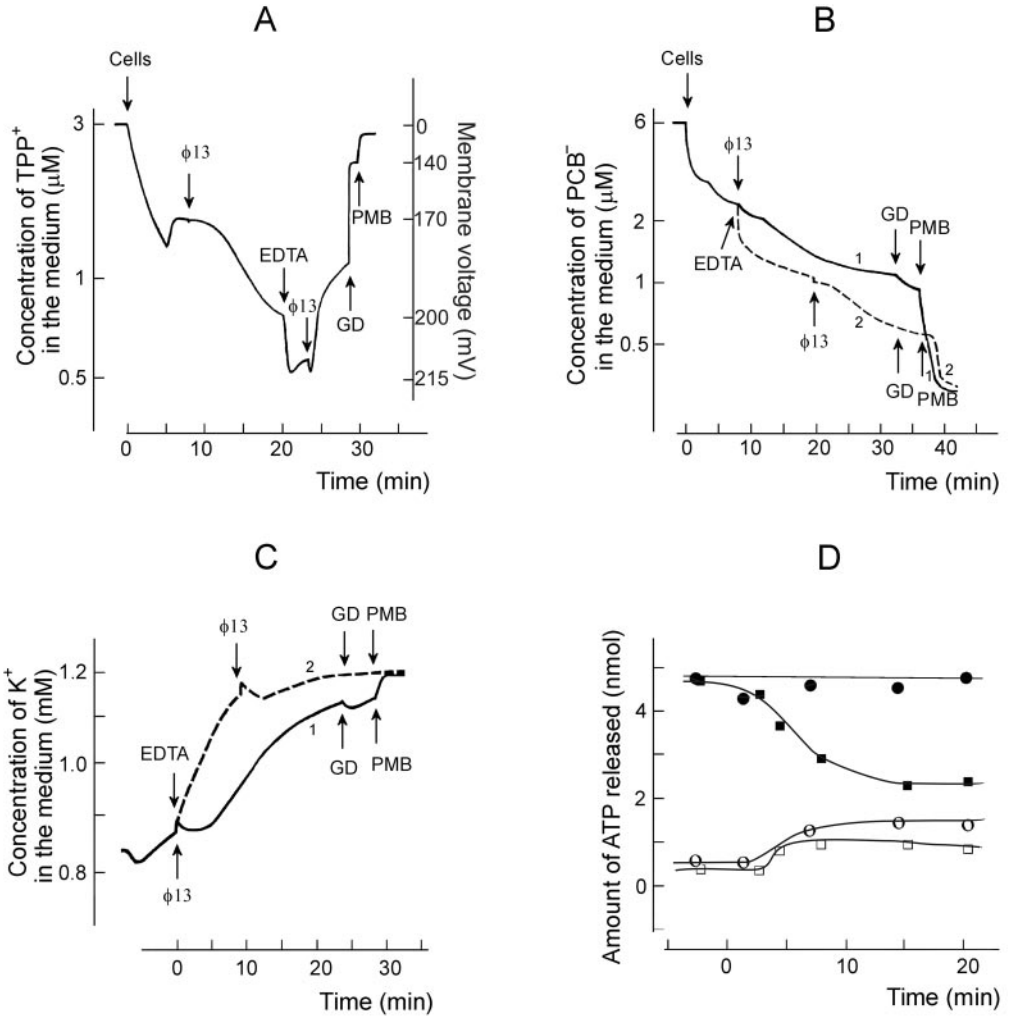

FIG. 5. Phage and EDTA effects on TPP^+ (A), PCB^- (B), K^+ (C), and ATP (D) content of *P. syringae* cells. The experiments were performed at 28°C in 100 mM sodium phosphate buffer (pH 8.0). The cells were added to the final concentration of 10^9 cells/ml (A to C). Unlabeled phage ϕ13 particles were added to obtain an MOI of 10 after each addition (A to C). EDTA was added to the final concentration of 0.2 mM, and GD and PMB were added to the final concentrations of 4 and 100 μg/ml, respectively. The ATP measurements in panel D were performed as described in Materials and Methods. The cells were infected at time point "0." Open circles (ϕ6) and squares (ϕ13) indicate the amount of free ATP in the cell incubation medium, and the filled circles (ϕ6) and squares (ϕ13) indicate the total amount of ATP in the cell suspension. The amount of ATP shown corresponds to 10^9 of the cells.

shows that the entry prevention took place after the fusion but before the particle reached the PM, being in line that the penetration of the peptidoglycan layer is inactivated.

DISCUSSION

Phage ϕ6 binds to the sides of the pilus and is brought to the cell surface by pilus retraction. Consequently, since there are only one to two pili per cell, only a few particles eventually enter the cell regardless of the MOI used (4, 44). The retraction process is cell energy dependent (32), thus complicating the study of ϕ6 entry-associated energetic events in detail. In contrast, the LPS receptor of ϕ13 (36) allows the virus to bind randomly on the cell surface, leading to MOI-dependent entry events. The measured maximal number of irreversibly bound active ϕ13 particles was about 60 per cell (Fig. 1C) but, due to low specific infectivity, the actual number of particles may be higher. ϕ13 can enter to several unrelated bacteria (36), suggesting that host envelope proteins may not play a significant role during the entry. However, we assume that the LPS receptor used by ϕ13 is a vital component of the host cell and that its alteration may lead to cell death. Screening of 150 putative phage-resistant cell lines did not lead to any true ϕ13-resistant cells, whereas phage ϕ6 resistance was commonly obtained (results not shown).

Interestingly, when MOIs higher than 10 were used, reduction of the amplitude of infection-induced increase in fluorescence was detected for ϕ13 (Fig. 2B). In the case of ϕ6 (4), the irreversible step in the entry is considered to be the fusion of the viral membrane with the OM, linking the irreversible binding to the fusion event. However, there may be yet another step after the receptor binding and before the fusion that irreversibly binds the virus to the cell. The difference between the maximum number of particles bound (~60, Fig. 1C) and the

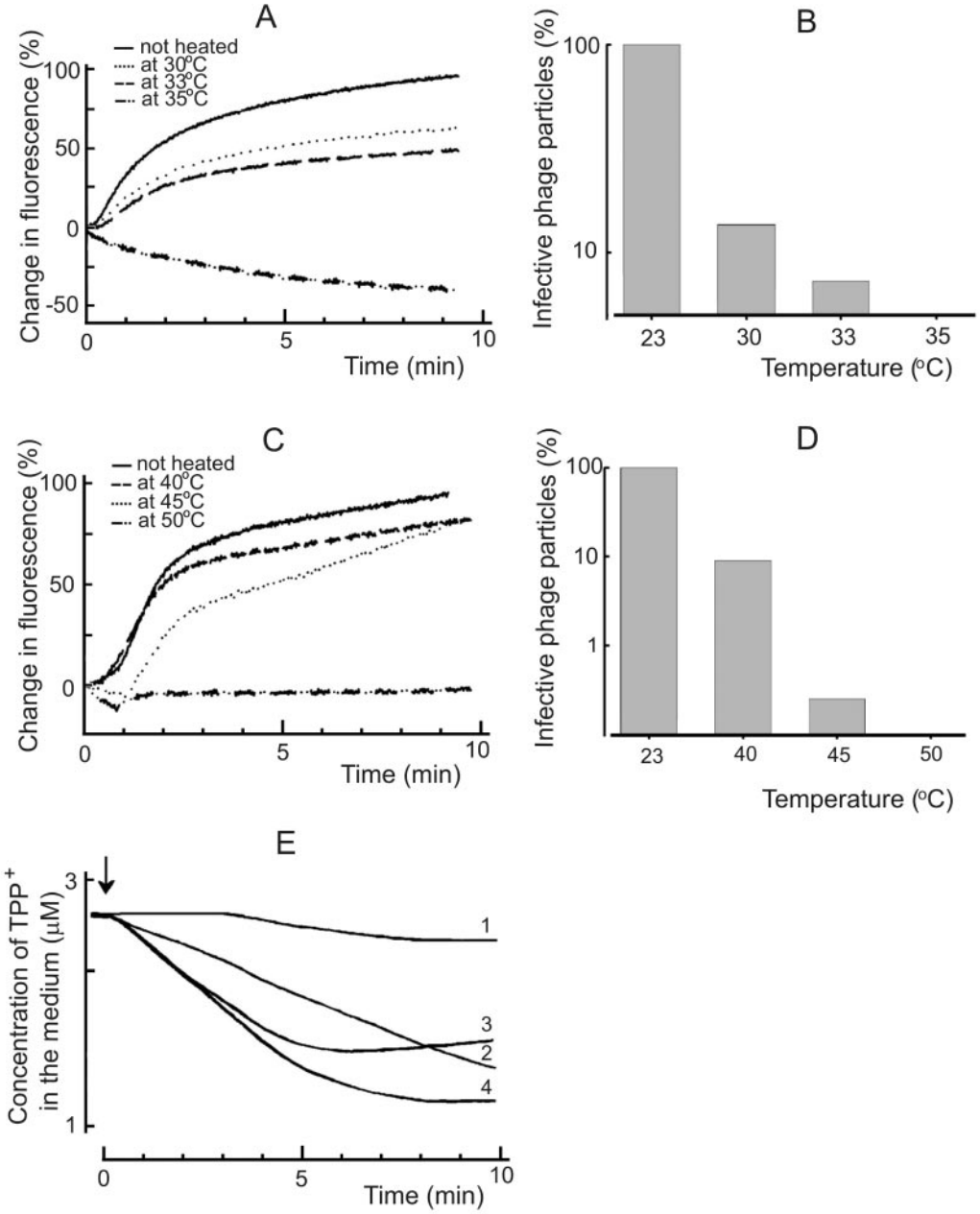

FIG. 6. Infection by heat-treated phage particles. Fusion kinetics were studied in 50 mM sodium phosphate buffer (pH 7.0) at room temperature. In the case of unheated phage ϕ13 (A) and ϕ6 (C) particles, the infection MOI was 10, and the same amounts of viruses were used after heating. The capability of the phage ϕ13 (B) and ϕ6 (D) particles to form infective centers was assayed after virus incubation at different temperatures for 10 and 15 min, respectively. (E) The TPP^+ uptake experiments were performed at 28°C in 50 mM sodium phosphate buffer (pH 7.0). The cells were added to obtain the final concentration of 2×10^8 CFU/ml. The MOI was 10 in the case of unheated phage infection, and the same amounts of particles were used after the heating. Curves: 1, HB10Y cells infected with unheated ϕ13; 2 and 3, LM2509 cells infected with ϕ13 heated for 10 min at 33 and 30°C, respectively; 4, LM2509 cells infected with unheated ϕ13. The arrow indicates the addition of phage.

number that cause a maximal increase in fluorescence (~10, Fig. 2B) suggests the presence of an irreversible binding step different from fusion. However, these measurements were performed under different conditions (no aeration during fluorescence measurements), possibly explaining some of the difference.

The ϕ13 adsorption/fusion is dependent on the physiological state of the cell. Inhibition of respiration rapidly renders the cells resistant to infection (Fig. 3A and C). The usage of high MOI also leads to the inhibition of fusion. The consequences of both of these events—blocked respiration and the increase of ion permeability of the PM after infection—are the depolarization of the PM and the decrease of H^+ concentration in the cell envelope (11, 13, 29). Depolarization of the PM by using incubation buffers with pH 6.0 prevented neither the irreversible binding of ϕ13 nor the infection-induced increase of the fluorescence (not shown). As in many animal viruses (21, 37), an acidic environment probably promotes the binding/

fusion of bacteriophages belonging to the *Cystoviridae* family. Since EDTA does not prevent infection-induced permeabilization of the membranes (Fig. 4 and 5) or increased fluorescence (not shown), divalent cations seem to be an unimportant factor for phage to traverse the OM.

It appears that in the ϕ13 system the irreversible binding is autoregulated by the number of infecting particles. When an increasing amount of phage particles interact with the host envelope, the PM permeability to H^+ increases above some threshold value and prevents the membrane fusion events. This is a superinfection immunity-related event (31) by using a unique mechanism.

A temporal increase of the OM permeability to lipophilic ions (TPP^+ and PCB^-) between ~1.5 and 4 min p.i. was observed (Fig. 4 and 5). This permeability coincided with the fast dilution of fluorophore-labeled virus-associated lipid molecules after infection (Fig. 2). These observations are in agreement with membrane fusion and the presence of temporal virus-derived membrane patches on the OM. The closure of the lipophilic ion-permeable window apparently occurs due to the lateral movement of LPS in the outer layer of the OM, closing the passage of lipophilic molecules (for a review, see reference 38).

Bacteriophage ϕ6 has a lytic enzyme, protein P5, associated with the NC surface (22). This enzyme is active after membrane fusion and digests an opening to the peptidoglycan layer (12, 35). Phage ϕ13 has a related protein, and we demonstrated here the presence of lytic activity associated with ϕ13 virions. It has been shown that P5 of ϕ6 is temperature sensitive (12), and the lytic protein of ϕ13 is also temperature sensitive, only more so (Fig. 6). This suggests that both ϕ6 and ϕ13 use a similar mechanism to penetrate the peptidoglycan layer.

Penetration of the ϕ6 NC through the PM is an endocytosis-like event that depends on membrane voltage (41). The NC penetration of ϕ6 was studied by using host cell spheroplasts (cells devoid of OM and peptidoglycan). This system was not optimal for studying the electrophysiology of the NC penetration due to the spontaneous leakage of intracellular indicator ions into the medium. Here we used intact cells and an MOI of 10 to assess the PM-associated events during ϕ6 and ϕ13 penetration (Fig. 4 and 5).

At 3 min p.i., K^+ ions were detected leaking from the cells in both the ϕ6 and the ϕ13 infections. However, this leakage was weak and gradually ceased at ca. 10 min p.i. Also, similar amounts of ATP leaked in both infections, but intracellular ATP concentrations continued to decrease in ϕ13-infected cells, whereas the ATP levels remained stable in the case of ϕ6 infection (Fig. 5D). We attribute these observations to the lower membrane voltage of ϕ13-infected cells (Fig. 4) that prevented ATP synthesis. Using an MOI of 10, the amplitudes of the virus-induced effects of ϕ13 are several times higher than those for ϕ6-infected cells. This is in line with different numbers of virus particles entering the cell.

In ϕ6 infection when only one to two particles enter the cell, the energy state of the host is not considerably altered. The PM is only slightly depolarized, and the intracellular ATP concentration is not considerably changed. In the case of ϕ13, MOIs higher than 10 had an adverse effect on virus production (not shown) and exhibited decreased entry-associated events (Fig. 2B). In addition, if the infected cells (MOI 10) were not aerated, lysis occurred (Fig. 1A). This suggests an active role of cell energy metabolism in repairing the infection-caused cell envelope defects.

Enveloped dsRNA bacterial viruses share entry principles (membrane fusion and PM penetration with an endocytosis-type mechanism) thought to occur only in animal viruses. This suggests that such mechanisms evolved early in the bacterial domain and were spread with the diversification of life.

ACKNOWLEDGMENTS

This study was supported by research grants 1202108 and 1202855 from the Academy of Finland (to D.H.B.; Finnish Center of Excellence Program [2000-2005]) and by Lithuanian State Science and Studies Foundation research grant 575 (to R.D.). R.D. is a Lithuanian State Fellowship holder. V.C. and E.B. were supported by EC project "Cebiola" (ICAI-CT-2000-70027).

REFERENCES

1. **Adams, M. H.** 1959. Bacteriophages. Interscience Publisher, Inc., New York, N.Y.
2. **Bamford, D. H., E. T. Palva, and K. Lounatmaa.** 1976. Ultrastructure and life cycle of the lipid-containing bacteriophage ϕ6. J. Gen. Virol. **32:**249–259.
3. **Bamford, D. H., and L. Mindich.** 1980. Electron microscopy of cells infected with nonsense mutants of bacteriophage ϕ6. Virology **107:**222–228.
4. **Bamford, D. H., M. Romantschuk, and P. J. Somerharju.** 1987. Membrane fusion in prokaryotes: bacteriophage ϕ6 membrane fuses with the *Pseudomonas syringae* outer membrane. EMBO J. **6:**1467–1473.
5. **Bamford, D. H., P. M. Ojala, M. Frilander, L. Wallin, and J. K. H. Bamford.** 1995. Isolation, purification, and function of assembly intermediates and subviral particles of bacteriophage PRD1 and ϕ6. Methods Mol. Genet. **6:** 455–474.
6. **Beveridge, T. J.** 1999. Structures of gram-negative cell walls and their derived membrane vesicles. J. Bacteriol. **181:**4725–4733.
7. **Blumenthal, R., S. A. Gallo, M. Viard, Y. Raviv, and A. Puri.** 2002. Fluorescent lipid probes in the study of viral membrane fusion. Chem. Phys. Lipids **116:**39–55.
8. **Boulanger, P., and L. Letellier.** 1988. Characterization of ion channels involved in the penetration of phage T4 DNA into *Escherichia coli* cells. J. Biol. Chem. **263:**9767–9775.
9. **Bradford, M. M.** 1976. A rapid and sensitive method for the quantification of microgram quantities of protein utilizing the principle of protein-dye binding. Anal. Biochem. **72:**248–254.
10. **Butcher, S. J., T. Dokland, P. M. Ojala, D. H. Bamford, and S. D. Fuller.** 1997. Intermediates in the assembly pathway of the double-stranded RNA virus ϕ6. EMBO J. **16:**4477–4487.
11. **Calamita, H. G., W. D. Ehringer, A. L. Koch, and R. J. Doyle.** 2001. Evidence that the cell wall of *Bacillus subtilis* is protonated during respiration. Proc. Natl. Acad. Sci. USA **98:**15260–15263.
12. **Caldentey, J., and D. H. Bamford.** 1992. The lytic enzyme of the *Pseudomonas* phage ϕ6: purification and biochemical characterization. Biochim. Biophys. Acta **1159:**44–50.
13. **Cherepanov, D. A., B. A. Feniouk, W. Junge, and A. Y. Mulkidjanian.** 2003. Low dielectric permittivity of water at the membrane interface: effect on the energy coupling mechanism in biological membranes. Biophys. J. **85:**1307–1316.
14. **Cuppels, D. A., A. K. Vidaver, and J. L. van Etten.** 1979. Resistance to bacteriophage ϕ6 by *Pseudomonas phaseolicola*. J. Gen. Virol. **44:**493–504.
15. **Daugelavičius, R., E. Bakiene, J. Berzinskiene, and D. H. Bamford.** 1997. Binding of lipophilic anions to microbial cells. Bioelectrochem. Bioenerget. **42:**263–274.
16. **Daugelavičius, R., J. K. H. Bamford, and D. H. Bamford.** 1997. Changes in host cell energetics in response to bacteriophage PRD1 DNA entry. J. Bacteriol. **179:**5203–5210.
17. **Daugelavičius, R., E. Bakiene, and D. H. Bamford.** 2000. Stages of polymyxin B interaction with *Escherichia coli* cell envelope. Antimicrob. Agents Chemother. **44:**2969–2978.
18. **Daugelavičius, R., E. Bakiene, J. Berzinskiene, and D. H. Bamford.** 2001. Use of lipophilic anions for estimation of biomass and cell viability. Biotechnol. Bioeng. **71:**208–216.
19. **Day, L. A., and L. Mindich.** 1980. The molecular weight of bacteriophage ϕ6 and its nucleocapsid. Virology **103:**376–385.
20. **Dimitrov, D. S.** 2004. Virus entry: molecular mechanisms and biomedical applications. Nat. Rev. Microbiol. **2:**109–122.
21. **Gaudin, Y., R. W. Ruigrok, and J. Brunner.** 1995. Low-pH induced conformational changes in viral fusion proteins: implications for the fusion mechanism. J. Gen. Virol. **76:**1541–1556.

22. **Hantula, J., and D. H. Bamford.** 1988. Chemical crosslinking of bacteriophage ϕ6 nucleocapsid proteins. Virology **165:**482–488.
23. **Henry, T., S. Pommier, L. Journet, A. Bernadac, J.-P. Gorvel, and R. Lloubes.** 2004. Improved methods for producing outer membrane vesicles in gram-negative bacteria. Res. Microbiol. **155:**437–446.
24. **Hoekstra, D., T. de Boer, K. Klappe, and J. Wilschut.** 1984. Fluorescence method for measuring the kinetics of fusion between biological membranes. Biochemistry **23:**5675–5681.
25. **Kakitani, H., H. Iba, and Y. Okada.** 1980. Penetration and partial uncoating of bacteriophage ϕ6 particle. Virology **101:**475–483.
26. **Kalasauskaite, E. V., D. L. Kadisaite, R. J. Daugelavičius, L. L. Grinius, and A. A. Jasaitis.** 1983. Studies on energy supply for genetic process: requirement for membrane potential in *Escherichia coli* infection by phage T4. Eur. J. Biochem. **130:**123–130.
27. **Keller, P. M., S. Person, and W. Snipes.** 1977. A fluorescence enhancement assay of cell fusion. J. Cell Sci. **28:**167–177.
28. **Kenney, J. M., J. Hantula, S. D. Fuller, L. Mindich, P. M. Ojala, and D. H. Bamford.** 1992. Bacteriophage ϕ6 envelope elucidated by chemical crosslinking, immunodetection, and cryoelectron microscopy. Virology **190:**635–644.
29. **Koch, A. L.** 1986. The pH in the neighborhood of membranes generating a protonmotive force. J. Theor. Biol. **120:**73–84.
30. **Loyter, A., V. Cytovsky, and R. Blumenthal.** 1988. The use of fluorescence dequenching measurements to follow viral membrane fusion events. Methods Biochem. Anal. **33:**129–164.
31. **Lu, M. J., and U. Henning.** 1994. Superinfection exclusion by T-even-type coliphages. Trends Microbiol. **2:**137–139.
32. **Maier, B., L. Poter, M. So, H. S. Seifert, and M. P. Sheetz.** 2002. Single pilus motor forces exceed 100 pN. Proc. Natl. Acad. Sci. USA **99:**16012–16017.
33. **Marvin, H. J. P., M. B. A. ter Beest, D. Hoekstra, and B. Witholt.** 1989. Fusion of small unilamellar vesicles with viable EDTA-treated *Escherichia coli* cells. J. Bacteriol. **171:**5268–5275.
34. **Mindich, L., J. F. Sinclair, and J. Cohen.** 1976. The morphogenesis of bacteriophage ϕ6: particles formed by nonsense mutants. Virology **75:**224–231.
35. **Mindich, L., and J. Lehman.** 1979. Cell wall lysin as a component of the bacteriophage ϕ6 virion. J. Virol. **30:**489–496.
36. **Mindich, L., X. Qiao, J. Qiao, S. Onodera, M. Romantschuk, and D. Hoogstraten.** 1999. Isolation of additional bacteriophages with genomes of segmented double-stranded RNA. J. Bacteriol. **181:**4505–4508.
37. **Mittal, A., E. Leikina, J. Bentz, and L. V. Chernomordik.** 2002. Kinetics of influenza hemagglutinin-mediated membrane fusion as a function of technique. Anal. Biochem. **303:**145–152.
38. **Nikaido, H.** 2003. Molecular basis of bacterial outer membrane permeability revisited. Microbiol. Mol. Biol. Rev. **67:**593–656.
39. **Olkkonen, V. M., and D. H. Bamford.** 1989. Quantitation of the adsorption and penetration stages of bacteriophage ϕ6 infection. Virology **171:**229–238.
40. **Peisajovich, S. G., and Y. Shai.** 2002. New insights into the mechanism of virus-induced membrane fusion. Trends Biochem. Sci. **27:**183–190.
41. **Poranen, M., R. Daugelavičius, P. M. Ojala, M. W. Hess, and D. H. Bamford.** 1999. A novel virus-host cell membrane interaction: membrane voltage-dependent endocytic-like entry of bacteriophage ϕ6 nucleocapsid. J. Cell Biol. **147:**671–681.
42. **Poranen, M. M., R. Daugelavičius, and D. H. Bamford.** 2002. Common principles in viral entry. Annu. Rev. Microbiol. **56:**521–538.
43. **Qiao, X., J. Qiao, S. Onodera, and L. Mindich.** 2000. Characterization of ϕ13, a bacteriophage related to ϕ6 and containing three dsRNA genomic segments. Virology **275:**218–224.
44. **Romantschuk, M., and D. H. Bamford.** 1985. Function of pili in bacteriophage ϕ6 penetration. J. Gen. Virol. **66:**2461–2469.
45. **Romantschuk, M., and D. H. Bamford.** 1986. The causal agent of halo blight in bean, *Pseudomonas syringae* pv. phaseolicola, attaches to stomata via its pili. Microb. Pathog. **1:**139–148.
46. **Romantschuk, M., V. M. Olkkonen, and D. H. Bamford.** 1988. The nucleocapsid of bacteriophage ϕ6 penetrates the host cytoplasmic membrane. EMBO J. **7:**1821–1829.
47. **Sambrook, J., and D. W. Russell.** 2001. Molecular cloning: a laboratory manual, 3rd ed. Cold Spring Harbor Laboratory Press, Cold Spring Harbor, N.Y.
48. **Smith, A. E., and A. Helenius.** 2004. How viruses enter animal cells. Science **304:**237–242.
49. **Stegmann, T., P. Schoen, R. Bron, J. Wey, I. Bartoldus, A. Ortiz, J. L. Nieva, and J. Wilschut.** 1993. Evaluation of viral membrane fusion assays. Comparison of the octadecylrhodamine dequenching assay with the pyrene excimer assay. Biochemistry **32:**11330–11337.
50. **Vidaver, A. K., R. K. Koski, and J. L. van Etten.** 1973. Bacteriophage ϕ6: lipid-containing virus of *Pseudomonas phaseolicola*. J. Virol. **11:**799–805.
51. **Yang, H., E. V. Makeyev, S. J. Butcher, A. Gaidelyte, and D. H. Bamford.** 2003. Two distinct mechanisms ensure transcriptional polarity in double-stranded RNA bacteriophages. J. Virol. **77:**1195–1203.